Available online at www.sciencedirect.com

SciVerse ScienceDirect

Advances in Space Research 52 (2013) 656–667

ADVANCES IN SPACE RESEARCH (a COSPAR publication)

www.elsevier.com/locate/asr

Analysis of precipitable water vapor from GPS measurements in Chengdu region: Distribution and evolution characteristics in autumn

Hao Wang [a,b,*], Ming Wei [a,b], Guoping Li [c], Shenghui Zhou [a,b], Qingfeng Zeng [a,b]

[a] Key Laboratory of Meteorological Disaster of Ministry of Education, Nanjing University of Information Science &Technology, # 219 Ningliu Road, Nanjing, Jiangsu 210044, China

[b] State Key Laboratory of Severe Weather, Chinese Academy of Meteorological Sciences, # 219 Ningliu Road, Nanjing, Jiangsu 210044, China

[c] College of Atmospheric Sciences, Chengdu University of Information Technology, # 24 Xuefu Road, Chengdu, Sichuan 610225, China

Received 24 January 2012; received in revised form 3 April 2013; accepted 4 April 2013
Available online 21 April 2013

Abstract

The rainfall process of Chengdu region in autumn has obvious regional features. Especially, the night-time rain rate of this region in this season is very high in China. Studying the spatial distribution and temporal variation of regional atmospheric precipitable water vapor (PWV) is important for our understanding of water vapor related processes, such as rainfall, evaporation, convective activity, among others in this area. Since GPS detection technology has the unique characteristics, such as all-weather, high accuracy, high spatial and temporal resolution as well as low cost, tracking and monitoring techniques on water vapor has achieved rapid developments in recent years. With GPS–PWV data at 30-min interval gathered from six GPS observational stations in Chengdu region in two autumns (September 2007–December 2007 and September 2008–December 2008), it is revealed that negative correlations exist between seasonally averaged value of GPS–PWV as well as its variation amplitude and local terrain altitude. The variation of PWV in the upper atmosphere of this region results from the water vapor variation from surface to 850 hPa. With the help of Fast Fourier Transform (FFT), it is found that the autumn PWV in Chengdu region has a multi-scale feature, which includes a seasonal cycle, 22.5 days period (quasi-tri-weekly oscillation). The variation of the GPS–PWV is related to periodical change in the transmitting of the water vapor caused by zonal and meridional wind strengths' change and to the East Asian monsoon system. According to seasonal variation characteristics, we concluded that the middle October is the critical turning point in PWV content. On a shorter time scale, the relationship between autumn PWV and ground meteorological elements was obtained using the composite analysis approach.

Keywords: Global positioning system (GPS); Precipitable water vapor; Fast Fourier Transform; Autumn rain; Composite analysis

1. Introduction

As the main greenhouse gas, water vapor in the atmosphere not only affects the global climate and weather but also plays a very important role in global heat and water cycles (Duan et al., 1996; Kiehl and Trenberth, 1997). It is therefore necessary to obtain the distribution condition of water vapor in the atmosphere and to understand the effects of spatial–temporal variation of water vapor on meso- and micro-scale severe weathers' evolution and on

* Corresponding author at: Key Laboratory of Meteorological Disaster of Ministry of Education, Nanjing University of Information Science and Technology, # 219 Ningliu Road, Nanjing, Jiangsu 210044, China. Tel.: +86 025 86531438; fax: +86 025 58699771.

E-mail addresses: wanghao911@163.com (H. Wang), mingwei@nuist.edu.cn (M. Wei), liguoping@cuit.edu.cn (G. Li), general_321@126.com (S. Zhou), Zengqing0419@sina.com (Q. Zeng).

0273-1177
http://dx.doi.org/10.1016/j.asr.2013.04.005

global climate change. GPS meteorology (or GPS/MET) rapidly developed in the 1990s, GPS–PWV (GPS–precipitable water vapor) retrieved from GPS technology has had wide and important applications in the related meteorology fields. The variation of GPS–PWV stands for the water vapor budget in the air column above the area. It is useful for weather forecasters to understand water vapor evolution conditions so that they know more about the weather process in this region, such as rainfall, evaporation, convective activity, among others (Fontaine et al., 2003).

Compared to the traditional detection means, GPS has more advantages in obtaining water vapor from the atmosphere, such as high accuracy, high capacity, high spatial and temporal resolution, all-weather, near-real time, and low cost, among others (Bevis et al., 1994; Ware et al., 2000). Moreover, GPS–PWV has been certified to have the same accuracy for deriving water vapor data with microwave radiometer, the very long baseline interferometry (VLBI) and radiosondes (Rocken et al., 1993; Bevis et al., 1994; Emardson et al., 1998; Van Baelen et al., 2005). Therefore, GPS technology has drawn meteorologists' attention in recent years. At present, it is mainly used for short-term and disastrous weather forecasting, and as an independent data source for data assimilation.

Located in the east of Qinghai-Tibet Plateau and the middle of the Sichuan Basin, Chengdu region belongs to the subtropical monsoon climate and is obviously affected by the topography. Especially in autumn, the convergence of humidity, convective activity and the diurnal cycle of rainfall in this area are very regional and have typical characteristics of the basin. Owing in part to the subtropical monsoon and the warm-humid climate, nighttime rainfall in this region is very high (Guo and Li, 2009; Li, 2011). So it is necessary to study deeply the local climate within peculiar topographic situations and further to find the mechanism of rainfall in this region. In the past, many researchers have shown the precipitation distribution and its variation characteristics in this area (Feng and Guo, 1983; Xu and Lin, 1994; Bai and Dong, 2004), but only a few studies are on spatial distribution of PWV or on the factors influencing the occurrence time and intensity of autumn rainfall. Additionally, most of these studies are based on the radiosonde data (Zhai and Eskridge, 1997). Because the radiosonde technology is non-uniform in terms of station allocation and is not so good in temporal resolution (only two soundings a day) and lack of continuity about the data, research on highly variable characteristics of water vapor and rainfall mechanism related to small scale is difficult. Though Shuanggen et al. (2008a) analyzed the GPS–PWV variation over China, but the source and formation mechanism of rainfall that have obvious regional features were not well discussed; in addition, the resolution of GPS–PWV they used was 2-h interval.

In recent years, the observational network of GPS/MET (including cooperative construction with Earthquake Administration, Surveying and Mapping Administration, Astronomical Observatory and Surveying and Investigation Institute) caught great attention from the meteorological departments throughout China. Regional ground-based GPS observational networks have been established in many places. In July 2007, the Chengdu Meteorological Bureau (hereinafter referred to as the CWB) and Chengdu Institute of Survey and Investigation (hereinafter referred to as CISI) set up six GPS observational network stations (Fig. 1); they are stations Chengdu (CDKC), Dujiangyan (DUJY), Jintang (JITA), Longquan (LOQU), Dayi (DAYI) and Pujiang (PUJI). The six stations are well distributed in the Chengdu plain. The longest baseline is 75 km from PUJI to LOQU, and the shortest baseline is 15.5 km from LOQU to CDKC. The 30-min interval GPS–PWV data gathered from the six GPS observational stations in this network in two autumns (September–December 2007 and September–December 2008) is used in this study, which mainly discusses the distribution characteristics and variation tendency of autumn PWV and the relationship between autumn PWV and ground meteorological elements. The data and analytical method is presented in Sections 2 and 3 is results and discussion and the conclusions are shown in final section.

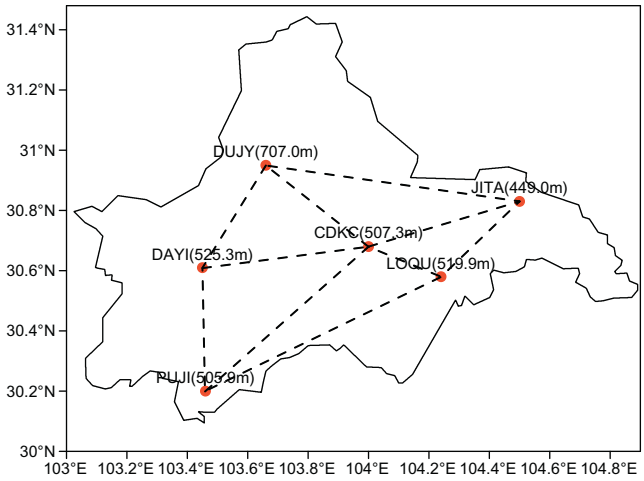

Fig. 1. Location of GPS stations (CHDC, LOQU, JITA, DUJY, DAYI, and PUJI) in Chengdu region. The number after each station name is the altitude of each GPS station.

2. Data and analysis

When GPS satellite lunches the radio wave through the atmosphere, the wave will be affected by the ionosphere and troposphere, thus its signals are delayed. This delay defined as the difference of signal propagation path between practicality and vacuum, which is a main factor influencing the accuracy of measurement in geodetic. However, GPS meteorology just derives the meteorological information from the delay. The delay can be classified into ionospheric delay and tropospheric delay. The ionospheric delay can be removed by dual-band technology in ground-based GPS receivers. The total delay minus the delay

caused by the ionosphere gives the troposphere delay, also named as the zenith total delay (ZTD), which is composed of zenith hydrostatic delay (ZHD) and zenith wet delay (ZWD). Thus, $ZTD = ZHD + ZWD$. Since the ZHD accounts for 90% of the ZTD, it can be obtained from an empirical model, such as the Saastamoinen model (Saastamoinen, 1972): $ZHD = 10^{-6}\frac{k_1 R p_s}{g_m M_d}$. Here, P_s is ground air pressure, R is ideal gas universal constant, M_d is molar mass of dry air, and M_d is gravity acceleration of vertical air column center. So we can estimate the ZHD from surface air pressure in this way. Then, we use the transformational relation formula $ZWD = \Pi \bullet PWV$ (Davis et al., 1985) to find PWV, where, Π is dimensionless water vapor conversion coefficient, $\Pi = \frac{10^6}{\rho_w R_v[(k_3/T_m)+k_2']}$, and ρ_w is liquid state water consistency. $k_2' = k_2 - k_1\frac{R_d}{\rho_w}$, and k_1, k_2, k_3 is experiment data. In this paper, we respectively use $k_1 = 77.6\ \mathrm{k/hPa}$ (Bevis et al., 1994), $k_2 = 71.92\ \mathrm{k/hPa}$ (Boudouris, 1963), $k_3 = 3.754 \times 10^5\ \mathrm{k/hPa}$ (Boudouris, 1963)). T_m is the mean temperature of troposphere atmosphere. Bevis's empirical equation $T_m = 70.2 + 0.72T_s$ (Bevis et al., 1994), where T_s is surface air temperature. In order to greatly improve the precision of what GPS derived, we can also establish a T_m correction scheme according to local radiosonde data of many years (Guo et al., 2008). Fig. 2 is the process of deriving GPS PWV from GPS total delay (Wang and Li, 2011).

The data used in this study is obtained by the means "cooperative construction and shared information" of different departments. Firstly, based on the GPS original data, the CISI estimates the total delay value of zenith every 30 min using the Bernese GPS software (Version 4.2), which uses double differences in phase. By FTP, the value is sent to the specified server of CWB. Combining relevant meteorological data of surface weather stations, CWB uses zenith hydrostatic delay model and weighted mean temperature model of troposphere to estimate the PWV at the six GPS stations in Chengdu region.

In order to test the accuracy of the data, station CDKC's GPS–PWV data in the autumns of 2007 and 2008 are selected as the example, and to compare the GPS–PWV with the Radiosonde-PWV (or RS-PWV) at the same time. The RS-PWV is derived from the formula:

$$PWV = -\frac{1}{g}\int_{p=p_0}^{p=p_1} qdp \tag{1}$$

where q is the specific humidity of each layer (where levels are the surface, 925, 850, 700, 500, 400, 300, and 200 hPa), p_0 is surface pressure, and p_1 is pressure of tropopause. Because the lower troposphere contains the major portion of the PWV, the PWV in the layer from surface to 200 hPa is considered the total amount of water vapor (Zhai and Eskridge, 1997). The RS-PWV derived from radiosonde data comes from radiosonde station Wenjiang, which is nearby the GPS station. At present, the method below is usually used to check GPS–PWV's precision (Li et al., 2010), namely, using formula (2) and (3), where the MAE stands for the mean absolute error between GPS–PWV and RS-PWV and the RMSE stands for the root mean square error.

$$\mathrm{MAE} = \frac{\sum_{i=1}^{n}|\mathrm{PWV(GPS)}_i - \mathrm{PWV(RS)}_i|}{n} \tag{2}$$

$$\mathrm{RMSE} = \sqrt{\frac{\sum_{i=1}^{n}(\mathrm{PWV(GPS)}_i - \mathrm{PWV(RS)}_i)^2}{n}} \tag{3}$$

The summation is from $i = 1$ to $i = n$, where i is the sequence number of samples and n is the total number of samples in the study. The results show that the MAE is

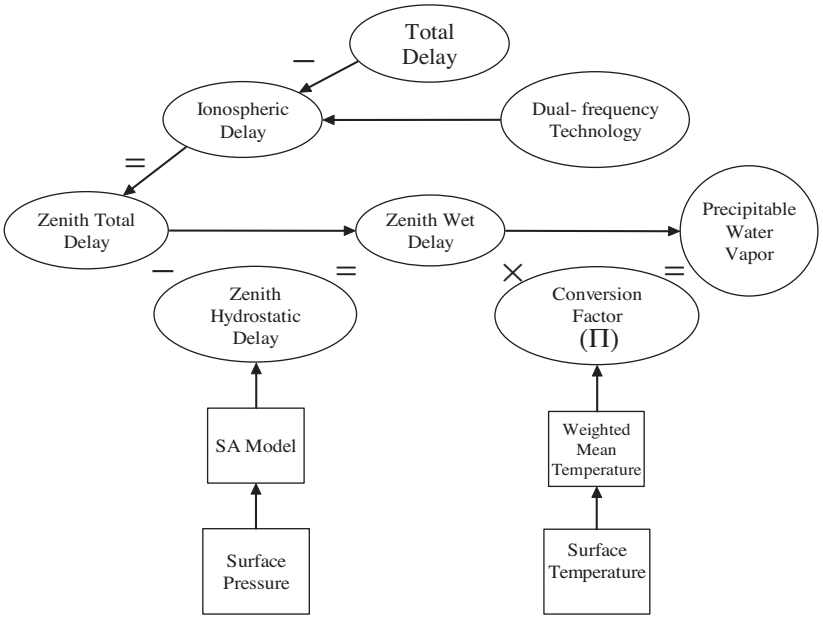

Fig. 2. Flow chart of deriving GPS–PWV from GPS total delay.

3.62 mm and the RMSE is 4.72 mm, which are in accord with the requirements of atmospheric research and business application (Li and Huang, 2004).

In order to see the variation characteristics of atmospheric water vapor in shorter time scales and to reveal the relationship between local climate characteristics and PWV, we choose stations CDKC and DAYI as examples, and study daily variation of relevant ground meteorological elements using composite analysis method (Li et al., 2008). In the autumns of 2007 and 2008, there was no strong rainfall process at stations CDKC and DAYI. It was a stable weather condition, and the circulation of water vapor was mainly controlled by local meteorological factors. Therefore, in the process of composite analysis, PWV and the corresponding ground meteorological elements are processed to mean diurnal data from the 182 days.

3. Results and discussion

3.1. Spatial distribution of GPS–PWV

The Chengdu regional GPS observational network provides 30-min interval GPS–PWV data with an information volume of over 8700 times at each station. To ensure that the non-uniformly distributed stations reflected the spatial correlation among the stations properly, linear variogram model of Kriging was used (Dingman et al., 1988) to interpolate the GPS–PWV data from the six stations (Table 1). Fig. 3(a) shows the spatial distribution of seasonally-averaged PWV. From this figure, it was found that the northwestern part of the Chengdu plain has the lower amounts of PWV, and the eastern part of the region has the higher amounts of PWV. In terms of the local terrain features, the Chengdu region is located in the east of the Qinghai-Tibet Plateau and in the middle of the Sichuan Basin. North of the Chengdu region are the Qinlin Mountains, and other mountains are present in the northwest as well. The altitude gradually drops across the Chengdu region from the northwest to the southeast. By comparing PWV and altitude, we found that the higher altitude GPS stations had the smaller PWV seasonal averages, and lower altitude GPS stations had much higher PWV values. Therefore, the two factors show a certain negative correlation. This relationship is shown in Fig. 3(b) and these findings are similar to what was observed by Shuanggen et al. (2008a) during their research on the spatial distribution of GPS–PWV throughout various locations in China.

We also observed a negative correlation between the altitude of the terrain and the standard deviation (SD) of the PWV data (Fig. 3(c) and (d). The value of SD can offer another perspective on the amplitude of variation of GPS–PWV of every station. In the relatively low altitude region of station JITA, the SD of PWV was 12.87 mm during the autumns. In contrast, SD of PWV in the autumns from the high altitude station DUJY was 9.45 mm.

In addition, the RS-PWV data of the 2 years was used to investigate the vertical distribution in this region; its features are all arc-like (Fig. 4(a) and (b), namely, at the same altitude the proportion that PWV accounts for the total PWV is relatively lower in the middle of the year while higher at the beginning and the end of the year, with the general range being rather small. Specifically speaking, in summer the main content of PWV can be distributed at a high level of the atmosphere while in winter more PWV is distributed at a lower level. It was found that the proportion in autumn is between summer's and winter's. By analyzing the PWV variation in autumn around Chengdu (surface-850, surface-700, and surface-500 hPa), we can get that the increase of PWV percentage in autumn mainly results from the water vapor variation exists between surface to 850 hPa (the increase of percentage was about 0.065% day^{-1} in 2007 and 0.107% day^{-1} in 2008), and that the water vapor contents from the surface to 700 and surface to 500 hPa are relatively stable, namely, with little variation (Fig. 5(a) and (b)). In this season, with the PWV at the same altitude showing an increasing tendency as time passes, the proportion that contained the PWV in every level accounts for the total PWV keeps growing. Therefore, the water vapor around Chengdu was gradually gathered at the low levels of the atmosphere after autumn comes, which creates favorable conditions for persistent precipitation in autumn.

3.2. Temporal variation of GPS–PWV

The variation of PWV is related not only to topographic features but also to seasonal variation and local character-

Table 1
Information of each station, including longitude, latitude, altitude, seasonally-averaged value and SD of GPS–PWV.

Station	Longitude (°)	Latitude (°)	Altitude (m)	Seasonally-averaged GPS–PWV (mm)	SD of GPS–PWV (mm)
CDKC	104.00	30.68	507.3	27.50	12.16
LOQU	104.24	30.58	519.9	28.27	12.50
DUJY	103.66	30.95	707.0	25.84	9.45
DAYI	103.45	30.61	525.3	28.61	11.33
PUJI	103.46	30.20	505.9	30.64	11.17
JITA	104.50	30.83	449.0	32.91	12.87

Note: The seasonally-averaged and SD of GPS–PWV was processed by GPS–PWV (30-min interval) of each station from September to November in both 2007 and 2008.

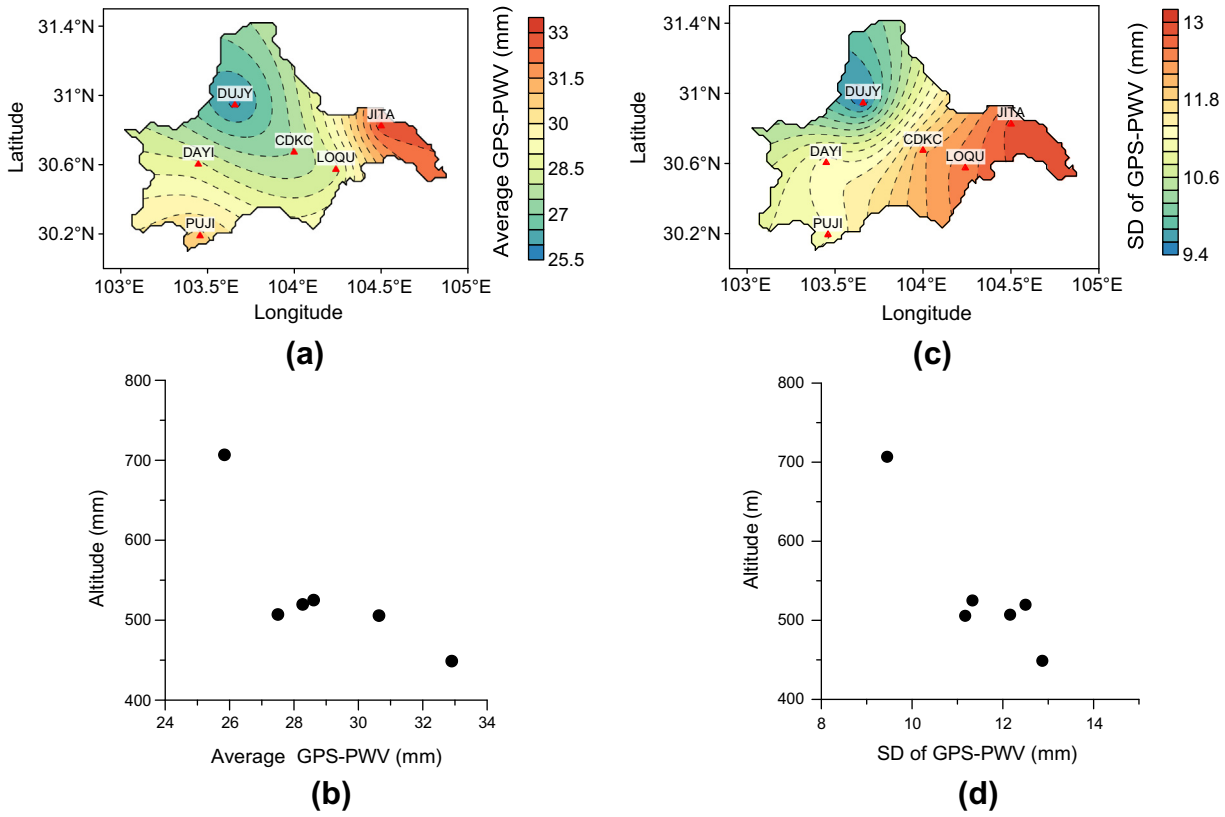

Fig. 3. Distribution (a) and relationship with altitude (b) of seasonally-averaged PWV in Chengdu region. The seasonally-averaged PWV was processed by GPS–PWV (30-min interval) from two autumns. Panels (c) and (d) are similar to (a) and (b), except the seasonally-averaged PWV has replaced by SD of PWV between the two autumns.

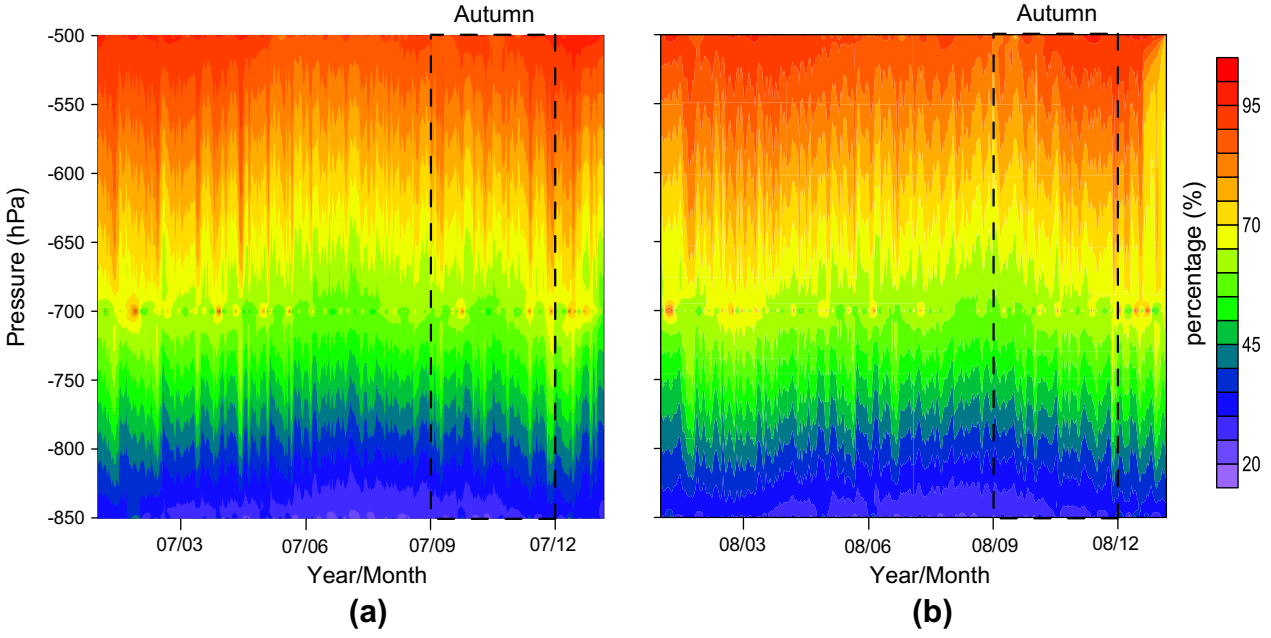

Fig. 4. Vertical distribution of PWV in station CDKC. The PWV data is from radiosonde station Wenjiang. Levels are the surface, 925, 850, 700, 500, 400, 300, and 200 hPa. Kriging interpolation method was used. Panels (a) and (b) are for Station CDKC in 2007 and 2008, respectively.

istics. By analyzing the time series of 30-min PWV in the two autumns from station CDKC (Fig. 6), we have learned that the GPS–PWV has the maximum value at the end of September or at the beginning of October and that the minimum value is at the end of December. It is also seen that there are several peaks in the time series of the GPS–PWV.

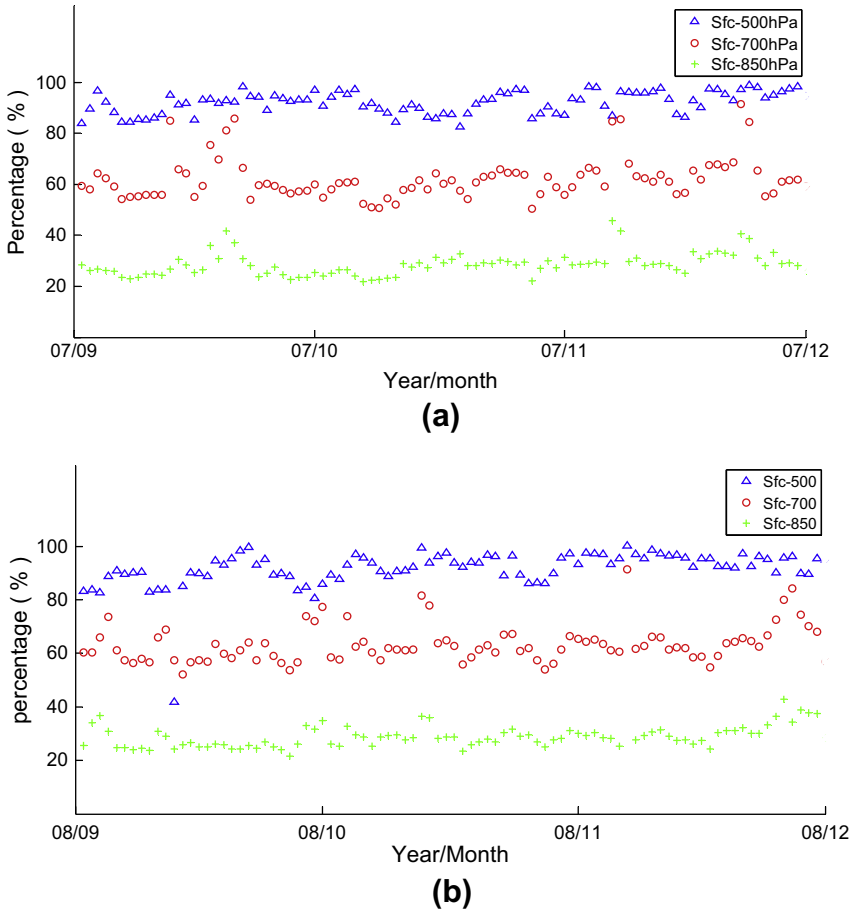

Fig. 5. Proportion of PWV accounted for the whole PWV at station CDKC on surface-850, surface-700, and surface-500 hPa. (a): 2007; (b): 2008. The largest rates of increase in percentage in Chengdu occur in surface to 850 hPa, the increase of percentage was about 0.065% day^{-1} in 2007 and 0.107% day^{-1} in 2008.

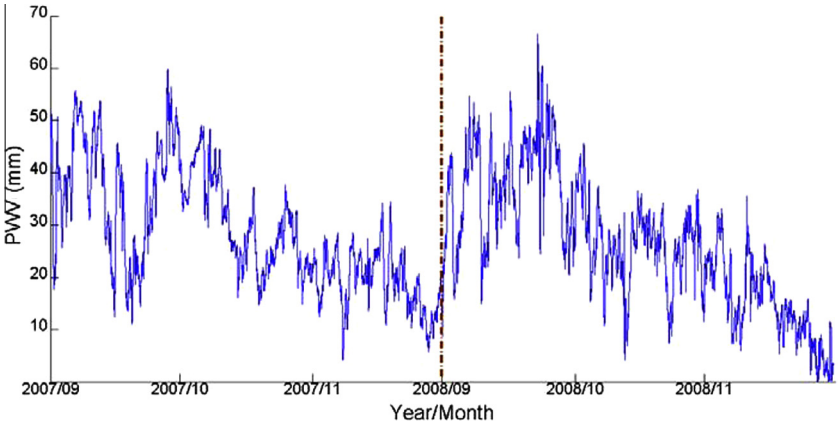

Fig. 6. PWV time series at station CDKC for September–November in 2007 and September–November in 2008.

Generally speaking, the PWV in every autumn shows the tendency of "a decline in the overall trend with local rise".

The FFT (Fast Fourier Transform) method is used to obtain the dominant periods of GPS–PWV in autumn. We find that the autumn PWV in the Chengdu region has a multi-scale feature, it has a seasonal cycle, plus a one quarter seasonal cycle, which is around 22.5 days or so (quasi-tri-weekly oscillation; Fig. 7). The rest of the stations also have this feature. From the example of the time series of GPS–PWV in the autumn of 2007, it is easily found the variation features. By analyzing the variation in Fig. 8, the PWV value first went up and then went down, and repeated it; the maximum of the second cycle is almost the same as the first cycle. Therefore, the variation of the

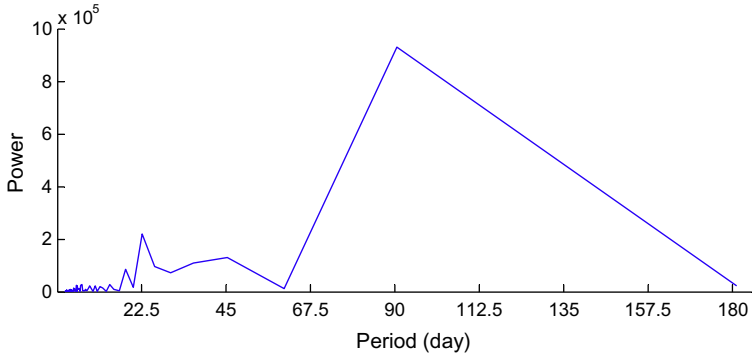

Fig. 7. Power spectra at Station CDKC using FFT for September–November in 2007 and September–November in 2008.

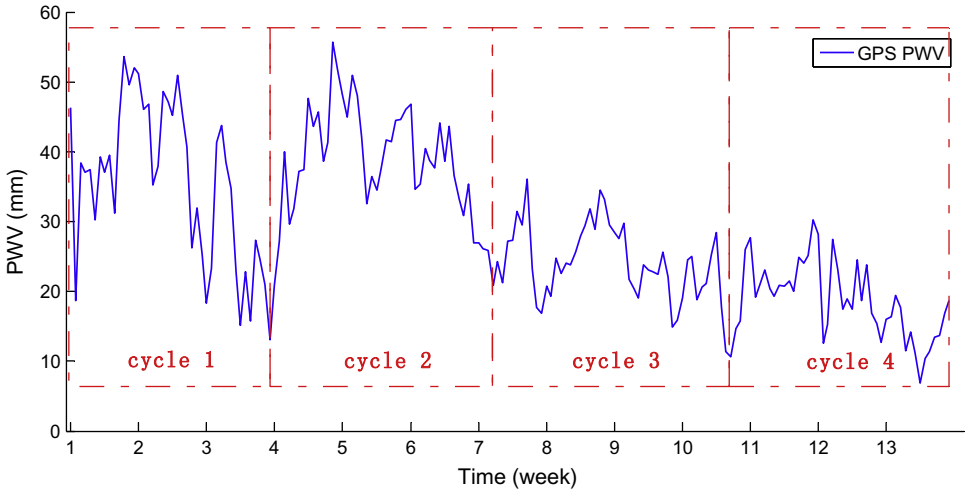

Fig. 8. Decomposed graph of cycle period of GPS–PWV at station CKDC (autumn 2007). The PWV value is obtained twice a day, at 8:00 a.m. (LST) and 20:00 p.m. (LST), respectively.

PWV in a longer period is about three weeks, with a turning in every seven days, although Cycles 3 and 4 are not very obvious because of the sharply declining PWV. The variation may be originated from periodical change in the transmitting of the water vapor caused by zonal and meridional wind strengths' change which has a particular periodicity (Wei and Ouyang, 2007, 2011). In Chengdu region, the PWV is very high in summer, lower PWV in winter. The water vapor sources of the Chengdu region is mainly from the South China Sea and the Bay of Bengal, so the meridional wind is an important carrier. If the zonal wind component is stronger, it will restrict the development of meridional wind component, thereby leading to a decrease of the PWV in this region. Zonal and meridional wind strengths' change results in the cyclical change of PWV. On the other hand, in summer, the monsoon system influences the East-Asia region and the prevailing southerly wind will bring large amount of water vapor to the mainland China. In winter, the northerly wind brings in cold and dry air (Huang et al., 2008). So the lower PWV in late autumn was influenced by the monsoon system. Combining the two points, we can conclude that the variation of the GPS–PWV is related to component wind strength's change and to the East Asian monsoon system.

By analyzing Fig. 9 with the average value of PWV in every cycle, we also know that stations CDKC, DAYI and JITA have the same changing tendency. To analyze the autumn GPS–PWV by comparing to the summer GPS–PWV, the PWV has an obvious decrease since the beginning of autumn and it reaches the minimum value at the end of autumn. If autumn is divided according to the quarter seasonal cycle period of Stages A, B, C, and D, we can find that the PWV maintained a relatively high value during Stages A and B. Since middle October, the PWV had a sudden decline. And compared with the PWV in Stage B, the PWV value in Stage C is decreased by nearly 30%, which shows that Stage C is the transition of PWV in autumn. It is consistent with the climatological characteristics of the Chengdu region, that is, there is more rain in early autumn, and there is little rain in late autumn.

3.3. Diurnal cycle of GPS–PWV

Before examine the composite diurnal features, it should be seen the diurnal variation using the entire two autumn's records. The GPS–PWV at stations CHDU and DAYI show two peak periods daily, namely, from 3:00 to 6:00 in the morning and from 15:00 to 22:00 in the afternoon

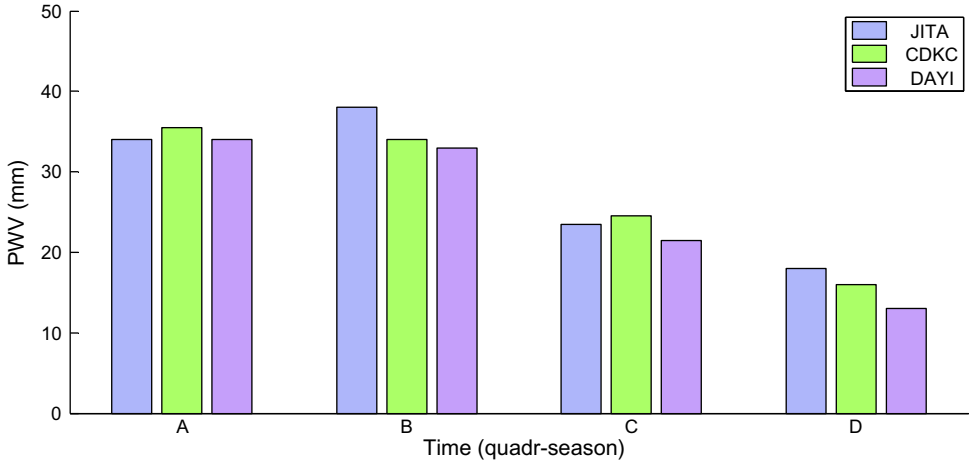

Fig. 9. PWV in every cycle period at three GPS stations (JITA, CDKC, and DAYI). The value of every cycle period was an average value of this period, which was processed by GPS–PWV (30-min interval) from the two autumns.

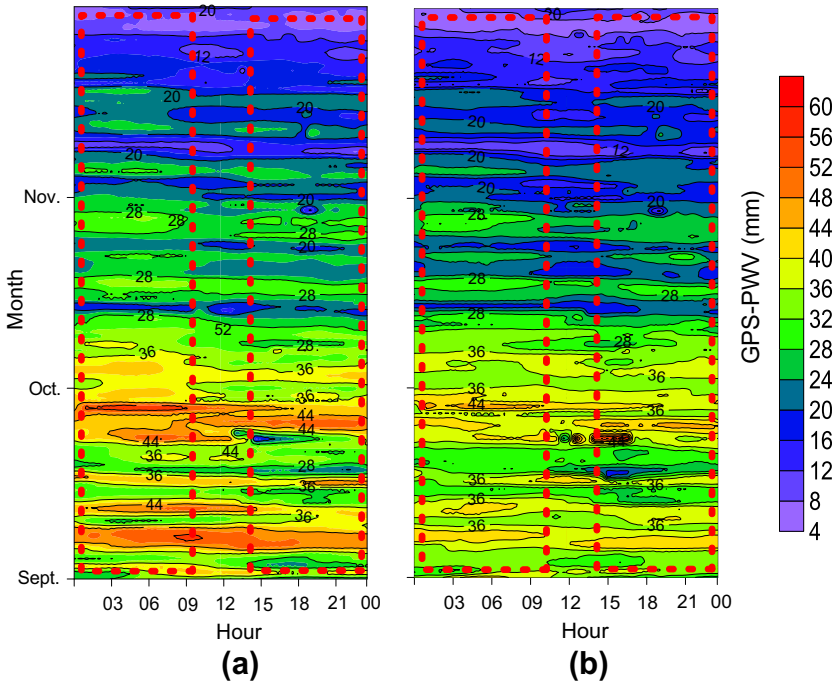

Fig. 10. Time series of diurnal variation of PWV at stations CHDU (left) and DAYI (right) during September–December 2007 and September–December 2008. The red box marks the high value center of each day.

and evening, with the second peak at station DAYI being more obvious (Fig. 10). The GPS–PWV also shows a wider variation range in September, and the characteristics of the two peak periods becomes more conspicuous during this month, with the maximum PWV appearing during the last 10 days of September at both stations. Shuanggen et al. (2008b) found that the diurnal and semidiurnal variations of ZTD were related to the atmospheric tidal force, but the correlation between PWV and tidal force needs to be further investigated.

From Fig. 11(a), we can see that the composite diurnal cycle characteristics of PWV at stations CDKC and DAYI are obvious. The PWV at station CDKC mainly has a weak double peak structure and station DAYI presents more distinct double peak feature, which may be due to the local climate differences. The PWV at both stations reaches the maximum in the morning, at 5:00 a.m. and 4:00 a.m., respectively, which illustrates the water vapor is not well distributed. At station CDKC, the maximum value at 5:00 a.m. reaches 29.2 mm, and the minimum at 6:30 p.m. is 26.3 mm. Combined with the diurnal cycle composite figure of actual precipitation based on ground meteorological data (Fig. 11(d)), we found that in the afternoon, the PWV for both stations showed a gradual upward

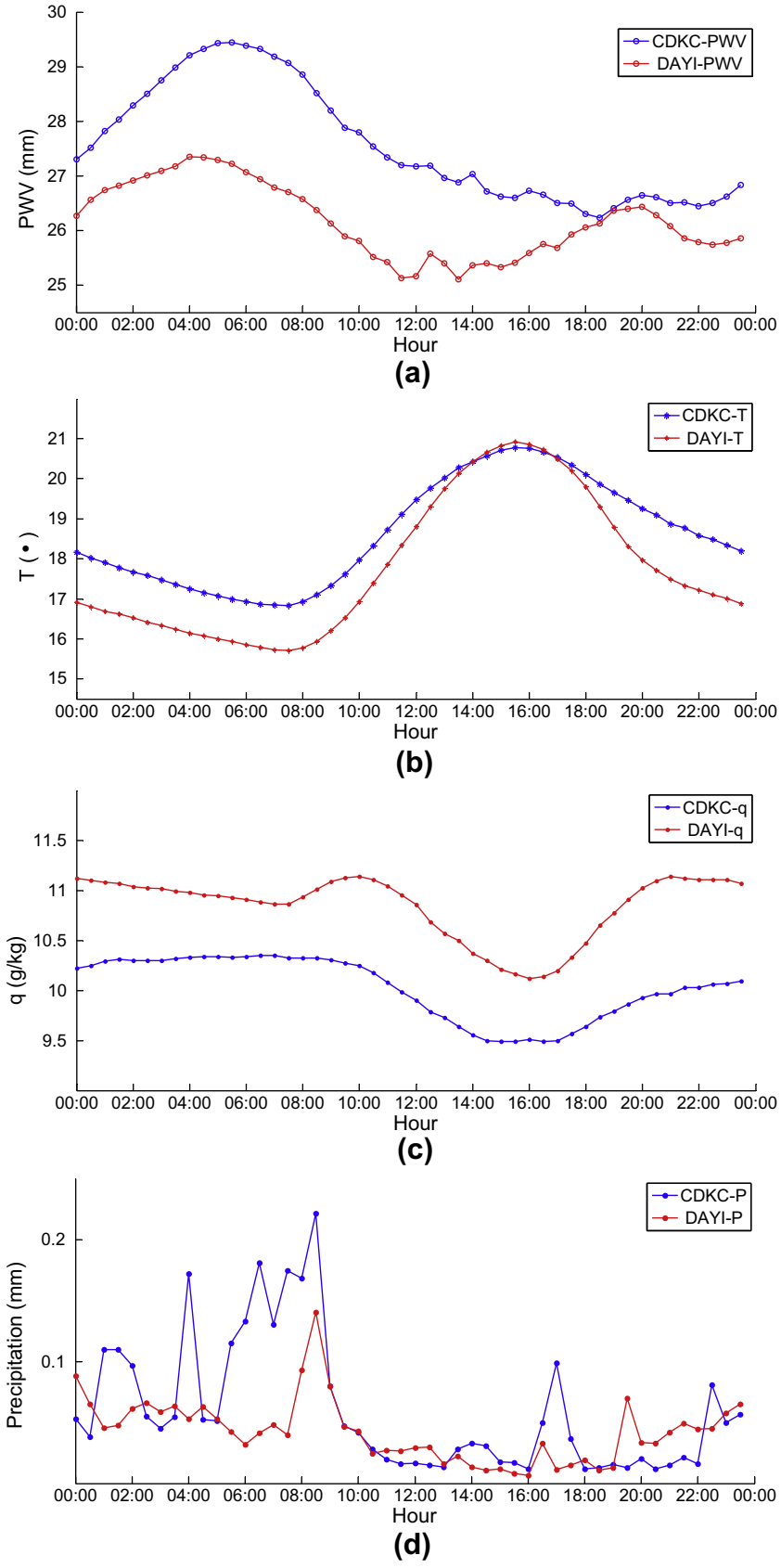

Fig. 11. Composite analysis on diurnal cycle at station CDKC and DAYI of PWV with related surface meteorological elements: (a) is PWV (mm) , (b) is temperature (°C), (c) is specific humidity (g/kg), and (d) is precipitation (mm).

trend of small magnitude. PWV amounts in the atmosphere were being accumulated, with typically low average precipitation levels. Between 00:00 and 05:00, there was a rapid increase in the amount of PWV, reaching a diurnal peak at about 05:00, but precipitation levels at this time did not exhibit any prominent changes. Over time, amounts of PWV decreased rapidly from the peak levels, in a sustained manner with a strong discharge. Conversely, precipitation levels increased continuously, reaching a daily maximum at about 08:00. There was a 3 h difference between the peaks of PWV and the peak of precipitation levels. From the above, it can be seen that a relatively long period of PWV accumulation, followed by a rapid increase before rainfall, are closely connected to the actual patterns of precipitation. Furthermore, a sustained increase in amounts of PWV before a sudden discharge indicates that there will be a significant change in precipitation levels. The time difference between the two events is an important point of reference, when making precipitation forecasts. Combined with the composite temperature (Fig. 11(b)), we can see that PWV has a negative correlation with temperature. Gaffen et al. (1992) showed that the relation between the variation of surface temperature and water vapor in the atmosphere also depends on the temperature range. The inherent relationship between temperature and PWV is complicated, and is difficult to demonstrate given the limited data for this study. The topic will, therefore, be further analyzed and researched in future studies. From the comparison of the variation characteristics and the variation of precipitable water in q (Fig 11(c)), e and RH (not shown, since e and RH have similar variation trends as q), the variation of q, e and RH has some inconsistency with the variation of PWV; that is, the timing of the highest and lowest values of e, q, and RH is different with that of PWV. The reason may be that after rainfall the increase of the moisture near the ground frequently falls behind the increase of the total water vapor. After the rainfall, the water vapor in the clouds has transformed into raindrops and fallen to the ground, and the total water vapor therefore decreases. What is more, after the rainfall the ground is moist, and the decrease of vapor pressure near the ground is often behind the decrease of the total water vapor. Therefore, because of the inconsistency of the atmospheric humidity variation between the upper and lower atmosphere, the timing of variation is not consistent among q, e, RH and PWV.

In general, a distinguishing feature of rainfall at stations CDKC and DAYI is that the rainfalls mainly happen in the night with the local sayings of "night rain in Bashan Mountain" and "Basin with more night rain." Such phenomena are caused by the unique local features combined with the wind in the basin. The temperature continues to go up from 8:00 a.m. to about 15:00 p.m., so the ground surface air mass is subject to sustained heating, thus comes about a strong convective motion, which causes the thermodynamic instability in the lower atmosphere. Additionally, the humidity near the ground surface always maintains a relatively high level in the morning and at night. At the same time, the PWV is rising and reaches its peak at night, because the temperature of troposphere is becoming lower and condensation appears easily at night. And the higher density and colder air at a higher location sinks along the edge of the basin to lift the warm and wet air at the lower location. All of these factors can cause the persistent rainfall at night. So, the thermodynamic and dynamic processes commonly affect the development of the rainfall process in this area. Kimura and Kuwagata (1995) reported that thermally induced local circulations play a vital role in the transport of heat and water vapor from plain to mountainous areas in a two-dimensional numerical model. Similar phenomenon was reported by Takagi and Kimura (2001) on the diurnal cycle in a deep valley over the Tibetan Plateau in 2000. They concluded that the daily maximum of PWV appears at mid-night, while the minimum shows up at 18:00 LST.

From Fig. 11, we can also find a corresponding relationship between the accumulating and releasing of PWV in the atmosphere and the actual rainfall process: The PWV maintaining sustained high level is the necessary condition of rainfall. For weather forecasting, the peak of the PWV is generally prior to the arrival of maximum value of rainfall intensity; therefore, the longer the high level PWV is sustained, the higher rainfall rate will follow. So, the rapid increase of GPS–PWV and its maintenance at a high level or greater deviation relative to average value of GPS–PWV in this season all have a good indication to the upcoming raining process.

4. Conclusions

Using GPS–PWV data of 30-min interval in the two autumns of 2007 and 2008 from the Chengdu ground-based GPS observational network, we obtained the space-time evolution characteristics of the autumn PWV in the Chengdu region. The results are summarized as follows.

1. Relationship between PWV and local terrain features: Distribution characteristics of PWV combined with local terrain features reveal the fact that the higher altitude, the smaller the average PWV, and vice versa.
2. Features of vertical distribution: In autumn, the PWV at the same altitude has an increasing tendency, the proportion that contains PWV accounts for the total PWV keeps growing and the variation of PWV in the upper atmosphere results mainly from the water vapor variation from surface to 850 hPa.
3. Relationship between PWV and season: The PWV in the Chengdu area not only has the seasonal variation feature, but also possesses the feature of 22.5 days or quasi-tri-weekly oscillation. The changes of PWV have a certain relationship with the strength of zonal and meridional wind as well as the East Asian monsoon sys-

tem. In the middle and the end of October, the value of PWV showed sharp decline. This period is the transition time of the PWV in autumn.

4. Relationship between PWV and local climate change: Through the analysis about the PWV variation features at stations CDKC and DAYI, it was found that the rainfall process mainly appears at the night or in the morning. The accumulating and releasing of PWV in the atmosphere have relatively good relationship with the actual rainfall process. In addition, the emergence time of the GPS–PWV peak is generally earlier than the emergence time of the maximum value of rainfall intensity, and the change of the PWV also has certain correlation with local e, q, RH, and T.

Through the research, we have further understanding of the variation feature of the autumn PWV in the Chengdu area. With the further increase of the GPS data, we will continue to deeply investigate the relationship between PWV and the periodical change of zonal and meridional wind strengths' change. Additionally, we plan to carry out chromatography assay of the ground-based GPS–PWV, and to calculate the slant PWV (SWV) to derive the vertical profile of atmosphere vapor. Not only can the vertical profile provide more detailed research data for studying the vapor variation mechanism but also offer 4D vapor variation information to forecasters; and consequently, we can realize the stereoscopic monitoring to the atmosphere water vapor in the Chengdu area and better serve the meteorological department and the society.

Acknowledgments

This work was supported by the Key University Scientific Research Project of Jiangsu Province (10KJA170030), The national basic research program of China (973 Program, 2013CB430102), Project of State Key Laboratory of Severe Weather of Chinese Academy of Meteorological Sciences (2010LASW-A01), Meteorology Industry Special Project of CMA (GYHY201306040), Nanjing weather radar open laboratory foundation (BJG201208), the National Natural Science Foundation of China (No. 41175045), the Special Fund for Meteorological Research in the Public Interest (No. GYHY201206042) and The Scientific Research Innovation Plan of College Graduate Student in Jiangsu Province (NO782002071). The authors would like to express their sincere thanks to the Chengdu Meteorological Bureau for supplying the GPS–PWV data. We thank reviewers for their constructive comments and editorial suggestions that significantly improved the quality of the paper.

References

Bai, Huzhi, Dong, Wenjie Climate features and formation causes of autumn rain over southwest China. Plateau. Meteor. 23 (6), 884–889, 2004.

Bevis, M., Businger, S., Chiswell, S., et al. GPS meteorology: mapping zenith wet delays onto precipitable water. J. Appl. Meteor. 33, 379–386, 1994.

Boudouris, G. On the index of refraction of air, the absorption and dispersion of centimeter waves in gases. Res. Natl. Bur. Stand. 67, 631–684, 1963.

Davis, J.L., Herring, T.A., Shaprio, I.I., et al. Geodesy by radio interferometry: effects of atmospheric modeling errors on estimates of baseline length. Radio Sci. 20, 1593–1607, 1985.

Dingman, S.L., Seely-Reynolds, D.M., Reynolds III, R.C. Application of Kriging to estimate mean annual precipitation in a region of orographic influence. Water Resour. Bull. 24, 329–339, 1988.

Duan, J., Bevis, M., Fang, P., et al. GPS meteorology: direct estimation of the absolute value of precipitable water. J. Appl. Met. 35, 830–838, 1996.

Emardson, T.R., Elegered, G., Johansson, J.M. Three months of continuous monitoring of atmospheric water vapor with a network of GPS receivers. J. Geophys. Res. 103, 1807–1820, 1998.

Feng, Liwen, Guo, Qiyun The fluctuation of autumn rain in South-West China. Geol. Res. 2 (1), 74–84, 1983.

Fontaine, B., Roucou, P., Trzaska, S. Atmospheric water cycle and moisture fluxes in the West African monsoon: mean annual cycles and relationship using NCEP/NCAR reanalysis. Geophys. Res. Lett. 30 (3), 1117, 2003.

Gaffen, D., Elliot, W.P., Robok, A. A. Relationship between tropospheric water vapor and surface temperature as observed radiosondes. Geophys. Res. Lett. 19, 1839–1879, 1992.

Jie, Gu, Li, Guoping, Huan, Dingfa Establish local model for weighted mean temperature of the troposphere based on 40a radiosonde data in Chengdu and Chongqing region. Geomat. Inf. Sci. Wuhan Univ. 33 (1), 43–46, 2008.

Guo, Jie, Li, Guoping Climatic characteristics of precipitable water vapor and relations to surface water vapor column in Sichuan and Chongqing region. J. Nat. Resour. 24 (2), 344–350, 2009.

Huang, Ronghui, Lei, Gu, Jilong, Chen, et al. Recent progresses in studies of the temporal–spatial variations of the East Asian monsoon system and their impacts on climate anomalies in China. Sci. Atmos. Sin. 32 (4), 691–719, 2008.

Van Baelen, Joël, Jean-Pierre, Aubagnac, Alain, Dabas Comparison of Near–Real time estimates of integrated water vapor derived with GPS, radiosondes, and microwave radiometer. J. Atmos. Oceanic Technol. 22, 201–210, 2005.

Kiehl, J.T., Trenberth, K.E. Earth's annual global mean energy budget. Bull. Am. Meteor. Soc. 78, 197–208, 1997.

Kimura, F., Kuwagata, T. Horizontal heat fluxes over complex terrain computed using a simple mixed-layer model and a numerical model. J. Appl. Meteor. 34, 549–558, 1995.

Li, Guoping Research of remote sensing technology of atmospheric water vapor by using ground-based GPS and application system of meteorological operations. Trans. Atmos. Sci. 34 (4), 385–392, 2011.

Li, Guoping, Huang, Dingfa Reviews and prospects of researches on remote sensing of regional atmospheric water vapor using ground-based GPS. Met. Sci. Technol. 32 (04), 201–205, 2004.

Li, Guoping, Huang, Dingfa, Guo, Jie, et al. Ground-based GPS Meteorology. M. Science Press, Beijing, 2010.

Li, G.P., Kimura, Fujio, Sato, Tomonori, et al. A composite analysis of diurnal cycle of GPS precipitable water vapor in central Japan during calm summer days. Theor. Appl. Clim. 92 (1–2), 15–29, 2008.

Rocken, C., Ware, R.H., Van Hove, T., et al. Sensing atmospheric water vapor with the global positioning system. Geophys. Res. Lett. 20, 2631–2634, 1993.

Saastamoinen, J., Atmospheric Correction for the Troposphere and Stratosphere in Radio Ranging of Satellites, C. American Geophysical Union, Washington, D.C., 1972.

Shuanggen, J., Li, Z., Cha, J. Integrated water vapor field and multiscale variations over China from GPS measurements. J. Appl. Meteor. Clim. 47, 3008–3015, 2008a.

Shuanggen, Jin, Luo, O.F., Gleason, S. Characterization of diurnal cycles in ZTD from a decade of global GPS observations. J. Geod. 83, 537–545, 2008b.

Takagi, T., Kimura, F. Diurnal variation of GPS precipitable water vapor at Lhasa in Premonsoon and Moosoon periods. J. Meteor. Soc. Jpn. 78, 175–180, 2001.

Wang, Hao, Li, Guoping Construction and application about the monitoring system of water vapor derived from ground-based GPS in Chengdu. J. Geog. Inf. Sci. 13 (2), 213–218, 2011.

Ware, R.H., Fulker, D.W., Stein, S.A., et al. SuomiNet: a real-time national GPS network for atmospheric research and education. Bull. Am. Met. Soc. 81, 677–694, 2000.

Wei, Ming, Ouyang, Shoucheng On subtropical anticyclone and high temperature drought in relation to the earth nutation and rotation. Eng. Sci. 9 (8), 40–46, 2007.

Wei, Ming, Ouyang, Shoucheng Characteristics of atmospheric structure and earth rotation of drought from winter in 2008 to spring in 2009. Eng. Sci. 13 (1), 49–55, 2011.

Xu, Guiyu, Lin, Chunyu Survey on the causes and features of autumn rain in western China. Sci. Meteor. Sin. 14 (2), 149–154, 1994.

Zhai, P.M., Eskridge, R.E. Atmospheric water vapor over China. J. Clima. 10, 2643–2652, 1997.